

Calculation of Some Fourth-Order Diagrams in Nuclear Matter*

A. G. PETSCHKE

University of California, Los Alamos Scientific Laboratory, Los Alamos, New Mexico

(Received 30 September 1963)

It is well known that in the Goldstone theory of many-fermion systems certain higher-order diagrams are included in the third-order diagrams if the hole self-energy is evaluated on the energy shell. In this paper a similar generalization of fourth-order diagrams is carried out. With this generalization, the Hartree-Fock potential U which cancels the third-order diagrams no longer cancels the fourth-order diagrams as well as before. The lack of cancellation is evaluated in two simple cases using the reference approximation, and found to be large in one case, small in the other.

IN the strict application of the theory of Goldstone¹ for many-fermion systems, irrelevant restrictions on the times of various interactions are imposed. The removal of these restrictions^{2,3} sometimes simplifies the calculation and always sheds light on its convergence. Consider the example given in BBP, the simple third-order diagram with a self-energy bubble on one hole line. In their notation and applying Goldstone theory strictly this bubble should be computed off the energy shell, in which case

$$\gamma^2 = m^* [2A + E_a + E_b - E_l - E_m] - k_0^2 \quad (1)$$

must be inserted into⁴

$$\langle k_0 | G^R | k_0 \rangle = 4\pi \left\{ \frac{1}{3} (\gamma^2 + k_0^2) c^3 + c(1 + \gamma c) \right\} \quad (2)$$

Since γ^2 depends on E_a and E_b this results in a large contribution to the Hartree-Fock energy of particles a and b . On the other hand, if the BrG scheme of evaluating this G on the energy shell is used, then

$$\gamma^2 = 2Am^* - k_0^2 \quad (3)$$

and there is no contribution to the energy of the particle lines. The difference can be regarded as either the result of summing an infinite set of diagrams or the result of removing an irrelevant restriction on the time ordering of the interactions. One sees that the lowest (3rd) order with the restriction is not a very good approximation, and that every hole self-energy should be evaluated on the energy shell.

A similar problem arises in fourth- and higher-order diagrams such as those given in Fig. 1 where it is unnatural to prevent two intermediate G matrices from overlapping in time. Consider for example the expansion of Fig. 1(a) in Fig. 2; it is clear that

$$t_b > t_\nu > t_{\nu-1} \cdots > t_1 > t_a \quad \text{and} \quad t_b > s_\mu > s_{\mu-1} \cdots > t_a \quad (4)$$

* Work done under the auspices of the U. S. Atomic Energy Commission.

¹ J. Goldstone, Proc. Roy. Soc. (London) **A293**, 276 (1957).

² K. A. Brueckner and D. T. Goldman, Phys. Rev. **117**, 207 (1960). Hereafter this paper is referred to as BrG.

³ H. A. Bethe, B. H. Brandow, and A. G. Petschek, Phys. Rev. **129**, 225 (1963). Referred to hereafter as BBP. The notation and the reference approximations introduced in BBP are used throughout the present paper.

⁴ A small correction term has been omitted from this formula.

but it is clearly undesirable to demand in addition that

$$t_1 > s_\mu \quad \text{or} \quad s_1 > t_\nu \quad (5)$$

as one normally would in Goldstone theory. An heuristic argument for the importance of removing the restriction (5) might be the following: if $t_1 > s_\mu$ the energy denominators between s_1 and t_ν are $2E$ once and $3E$, $\mu + \nu - 2$ times, where E is the difference in energy between a typical particle and a typical hole. Only one time order-

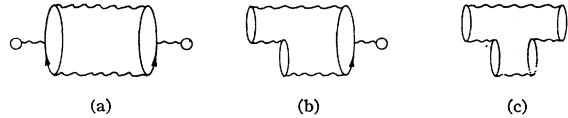


FIG. 1. Fourth-order diagrams in which two G matrices have the same constraints on interaction time.

ing of the interactions is possible. With the times interleaved, the energy denominators are $3E$, $\lambda + 2$ times and $4E$, $\mu + \nu - 3 - \lambda$ times, where λ is some positive integer. But now there are $(\mu + \nu)! / (\mu! \nu!)$ different orders. The number of different time orderings grows much more rapidly than the product of the energy denominators, and a simple calculation shows that the contribution excluded by the strict approach is equal to that included by the time $\mu = \nu = 2$. For these reasons it seems worthwhile to remove the restriction in general. To simplify the following discussion, no effort is made to evaluate a fourth-order diagram, only the second-order insertions into other diagrams are evaluated.

Let E_0 be the energy denominator after time t_a , δD_j the change in energy associated with time s_j and δE_j that associated with t_j . Then the product of the energy

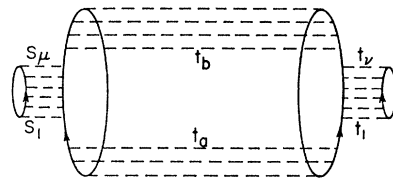


FIG. 2. Expansion in interactions of the potential of Fig. 1(a). The labels are the time of interaction and serve to fix the notation.

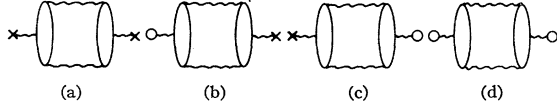


FIG. 3. Diagrams that should be treated with Fig. 1(a) if a Hartree-Fock potential U is used.

denominators between t_a and t_b is given by the following integral, which can be derived from the adiabatic approximation:

$$\begin{aligned} & \lim_{\alpha \rightarrow 0} (i\hbar)^{-\nu-\mu-1} \int_{-\infty}^{t_b} dt_a e^{it_a(E_0-i\alpha)/\hbar} \int_{t_a}^{t_b} dt_\nu \int_{t_a}^{t_\nu} dt_{\nu-1} \cdots \\ & \times \int_{t_a}^{t_2} dt_1 \prod_j e^{it_j(\delta E_j-i\alpha)/\hbar} \int_{t_a}^{t_b} ds_\mu \int_{t_a}^{s_\mu} ds_{\mu-1} \cdots \\ & \times \int_{t_a}^{s_2} ds_1 \prod_j e^{is_j(\delta D_j-i\alpha)/\hbar}. \quad (6) \end{aligned}$$

The order of integration has been changed slightly from the normal one to make it possible to impose the restrictions (4). Note that (5) is *not* imposed. It is easily seen that this integral has the right value if either μ or ν or both are zero. Since

$$\int_{-\infty}^{\infty} e^{i\epsilon(t_a-s_a)/\hbar} d\epsilon = 2\pi\hbar \delta(t_a-s_a)$$

the expression (6) can be written, changing the order of integration,

$$\begin{aligned} & \lim_{\alpha \rightarrow 0} \frac{(i\hbar)^{-\mu-\nu-1}}{2\pi\hbar} \int_{-\infty}^{\infty} d\epsilon \\ & \times \left\{ \int_{-\infty}^{t_b} dt_a e^{it_a(E_0-\epsilon-i\alpha)/\hbar} \int_{t_a}^{t_b} dt_\nu \cdots \right. \\ & \times \left. \int_{t_a}^{t_2} dt_1 \prod_j e^{it_j(\delta E_j-i\alpha)/\hbar} \right\} \\ & \times \left\{ \int_{-\infty}^{t_b} ds_a e^{is_a\epsilon/\hbar} \int_{s_a}^{t_b} ds_\mu \cdots \right. \\ & \times \left. \int_{s_a}^{s_2} ds_1 \prod_j e^{is_j(\delta D_j-i\alpha)/\hbar} \right\} \quad (7) \end{aligned}$$

where attention has been called, by the use of brackets, to the fact that the s and t integrations are now independent. The absence of a convergence factor from the s_a integration is clearly trivial. The energy denominators that will appear after the integrations in the brackets are just those that are necessary to calculate the two G 's, off the energy shell by an amount $E_0-\epsilon$ and ϵ respectively, and in addition two factors of $(E_0-\epsilon-i\alpha)^{-1}$

and two of $(\epsilon-i\alpha)^{-1}$. Instead of the Goldstone contribution

$$-2 \frac{1}{E_0} G_2(E_0) \frac{1}{E_0} G_3(E_0) \frac{1}{E_0} \quad (8)$$

one therefore gets

$$\begin{aligned} & \frac{i}{2\pi} \lim_{\alpha \rightarrow 0} \int_{-\infty}^{\infty} d\epsilon \frac{1}{(\epsilon-i\alpha)^2} \frac{1}{(E_0-\epsilon-i\alpha)^2} \\ & \times G_2(\epsilon-i\alpha) G_3(E_0-\epsilon-i\alpha), \quad (9) \end{aligned}$$

where the argument of G gives the distance from the energy shell.

Now

$$\gamma^2(E) = (E_0+A)m^* - k_i^2, \quad (10)$$

where k_1 or k_2 are the initial relative momenta in the intermediate G matrices. If only the "core volume" (first) term of (2), which is important for large E_0 , is used in G , then insertion into (8) gives

$$-\left(\frac{4\pi c^3 m^*}{3}\right)^2 \frac{2(A+E_0)^2}{E_0^3} \quad (11)$$

while integration of (9) gives

$$-\left(\frac{4\pi c^3 m^*}{3}\right)^2 \frac{E_0^2 + 2AE_0 + 2A^2}{E_0^3} \quad (12)$$

which is only about half as big. The diagram just discussed should be taken together with the three others in Fig. 3, in which one or both of the G 's are replaced by the Hartree-Fock potential $-U$. U itself is an average over the Fermi sea of $G(E_0)$. In Goldstone theory these diagrams differ only in sign, depending on the number of U 's involved. In the generalization the diagram with one U and one G becomes

$$\begin{aligned} & -G_2(E_0) \frac{i}{2\pi} \lim_{\alpha \rightarrow 0} \int_{-\infty}^{\infty} \frac{1}{(\epsilon-i\alpha)^2} \\ & \times \frac{1}{(E_0-\epsilon-i\alpha)^2} G_3(E_0-\epsilon-i\alpha) d\epsilon \\ & = +\left(\frac{4\pi c^3 m^*}{3}\right)^2 \frac{2A^2 + 3AE_0 + E_0^2}{E_0^3} \quad (13) \end{aligned}$$

while the diagram with only U interaction gives (11). The sum of the four diagrams is therefore

$$-\left(\frac{4\pi c^3 m^*}{3}\right)^2 \frac{1}{E_0} \quad (14)$$

while in Goldstone theory it would be exactly zero, and without a Hartree-Fock potential it would be (12), which is of the same order as (14).

If both terms in (2) are used for G , the sum of the four

diagrams in Fig. 3 becomes

$$\begin{aligned} & -\frac{16\pi^2}{E_0} \left[\frac{c^6 m^{*2}}{9} - \frac{2K_2 K_3}{E_0^2} + \frac{c^4 m^*}{2E_0} \left(\frac{K_3}{K_2} + \frac{K_2}{K_3} \right) + \frac{c^7 m^{*2}}{6} \right. \\ & \times \left(\frac{1}{K_2} + \frac{1}{K_3} \right) + \frac{c^4 m^*}{2\pi} \left\{ \frac{4}{E_0} + \left(\frac{4C}{E_0^2} + \frac{B}{E_0} \right) C^{-1/2} \tan^{-1} \frac{2C^{1/2}}{B} \right. \\ & \left. \left. + \left(\frac{4C'}{E_0^2} + \frac{B'}{E_0} \right) C'^{-1/2} \tan^{-1} \frac{2C'^{1/2}}{B'} \right\} \right], \quad (15) \end{aligned}$$

where

$$\begin{aligned} K_2 &= c^2 \{ P_2^2 + m^* (2A - E(k) - E(a) + E_0) \}^{1/2}, \\ K_3 &= c^2 \{ P_3^2 + m^* (2A - E(l) - E(b) + E_0) \}^{1/2}, \\ B &= (1/m^* c^4) (K_2^2 - K_3^2) + E_0, \\ B' &= (1/m^* c^4) (K_3^2 - K_2^2) + E_0, \\ C &= (1/m^{*2} c^8) (K_3^2 - m^* c^4 E_0) K_2^2, \\ C' &= (1/m^{*2} c^8) (K_2^2 - m^* c^4 E_0) K_3^2. \quad (16) \end{aligned}$$

Since the most important matrix elements of the hard core in the first G matrix give relative momenta $k_a = k_b = \pi/2c$ it is reasonable to take the initial relative momenta in G_2 and G_3 equal to $k_1 = \pi/4c$. In this case

$$E_0 = (4k_1^2/m) + 2A. \quad (17)$$

We simplify further by taking $A=0$ and $m^*=1$, since these parameters are not well established. The values of various expressions with this choice of parameters are given in Table I, both for the core volume term alone

TABLE I. Values of various expressions in the text.

	Core volume term only	All of expression (2)
Goldstone contribution (8)	$-14.2c^8$	$-220 c^8$
Residue, i.e., (14) or (15)	$-7.1c^8$	$-16.3c^8$

[the first part of (2)] and for all of G^R . The first row gives the Goldstone contribution, expression (8), which one hopes the Hartree-Fock potential will cancel. The second row gives the residual contribution as given by (14) or (15) of this paper. When the second row is small, as it is when all of G^R is used, the H-F potential is serving its function even in 4th order. When the second row is of the same order as the first, as with the core volume term, the H-F potential which cancelled the third-order diagrams exactly is not qualitatively decreasing the fourth-order diagrams.

Although the illustration may be somewhat artificial, since, as can be seen from the table, the core volume term is only a small part of the total hard-core contribution; it has been the purpose of this paper to show that rapid convergence of the Goldstone series⁶ is by no means assured by making the third-order diagrams small.

ACKNOWLEDGMENT

The author is grateful to the Physics Division of the Aspen Institute for Humanistic Studies for extending their hospitality while some of this work was done.

Average Number of Prompt Neutrons from U^{235} Fission Induced by Neutrons from Thermal to 8 MeV

D. S. MATHER, P. FIELDHOUSE, AND A. MOAT

Atomic Weapons Research Establishment, Aldermaston, Berks, England

(Received 21 October 1963)

A large, loaded-liquid scintillation counter has been used to measure the average number, $\bar{\nu}$, of neutrons emitted in the neutron-induced fission of U^{235} as a function of the incident energy. Time-of-flight techniques were employed where necessary to select fissions induced by neutrons of the desired energy. Values at nineteen energies in the range thermal to 8 MeV were determined; absolute values are based on $\bar{\nu}$ (Cf^{252} , spontaneous) = 3.782 ± 0.024 , relative errors are about 1%. The variation of $\bar{\nu}$ with energy cannot be represented by a single straight line. A satisfactory fit to the experimental points is given either by the relationship

$$\bar{\nu}(E) = (2.423 \pm 0.008) + (0.088 \pm 0.008)E + (0.0088 \pm 0.0011)E^2,$$

or by two straight lines

$$\begin{aligned} \bar{\nu}(E) &= (2.418 \pm 0.008) + (0.109 \pm 0.006)E \text{ from 0 to 3 MeV,} \\ \bar{\nu}(E) &= (2.200 \pm 0.023) + (0.181 \pm 0.005)E \text{ from 3 to 8 MeV.} \end{aligned}$$

I. INTRODUCTION

THE measurement of $\bar{\nu}$, the average number of neutrons emitted in fission, is important from both the practical and theoretical viewpoints. Calcula-

tions of the properties of fissile assemblies require precise knowledge of $\bar{\nu}$, while any proposed theory of fission must show how this parameter is related to the excitation, mass, and charge of the fissioning nucleus.